

# State switching in Bi-doped $\text{La}_{0.67}\text{Ca}_{0.33}\text{MnO}_3$ and the effects of current

J. R. Sun<sup>a)</sup>

Department of Physics, The University of Hong Kong, Pokfulam Road, Hong Kong and State Key Laboratory for Magnetism, Institute of Physics and Center for Condensed Matter Physics, Chinese Academy of Sciences, Beijing 100080, China

J. Gao and L. Kang

Department of Physics, The University of Hong Kong, Pokfulam Road, Hong Kong

(Received 29 April 2002; accepted for publication 17 May 2002)

Electronic transport and magnetic properties of  $\text{La}_{0.477}\text{Bi}_{0.193}\text{Ca}_{0.33}\text{MnO}_3$  have been experimentally studied. Different resistive behaviors are observed in the cooling and warming processes. The system first stays at a high resistive state, and switches to a state of lower resistivity when it is cooled below a critical temperature. However, keeping the sample at a temperature below  $\sim 60$  K, a relaxation to the high resistive state takes place. This process is current dependent, and the application of a large current slows down the relaxation greatly. There is a strong competition between the two resistive states, which causes a switch of the system between states. © 2002 American Institute of Physics. [DOI: 10.1063/1.1494109]

$\text{La}_{2/3}\text{Ca}_{1/3}\text{MnO}_3$  is a typical colossal magnetoresistance (CMR) material, in which a paramagnetic-to-ferromagnetic transition takes place accompanied by an insulation-to-metal (MI) transition, and the application of a magnetic field depresses the resistivity near  $T_c$  greatly, causing the CMR behavior.<sup>1-4</sup> However, partially replacing La by Pr or Nd produces a much more complex behavior.<sup>5,6</sup> In addition to the progressive suppression of the magnetic order, characterized by the reduction of  $T_c$  and magnetization, a two-step magnetic behavior occurs after a critical doping of Pr/Nd. Accordingly, the overall resistivity increases and the MI transition shifts to lower temperatures. Meanwhile, a visible resistivity jump develops in the  $\rho(T)$  curve with the increase of Pr/Nd content, indicating the occurrence of charge ordering (CO) that localizes the charge carrier. Metallic conduction disappears after a critical doping.

The rich and varied behavior of the Pr/Nd-doped compound can be understood in the scenario of phase separation due to the incorporation of Pr/Nd that causes a coexistence of the charge-ordered and ferromagnetic phases. A common feature of  $\text{Pr}_{1-x}\text{Ca}_x\text{MnO}_3$  and  $\text{Nd}_{1-x}\text{Ca}_x\text{MnO}_3$  is the CO transition.<sup>7</sup>  $\text{Bi}_{1-x}\text{Ca}_x\text{MnO}_3$  is similar to the above two systems in the sense that it also shows a strong tendency to CO.<sup>8</sup> However, when replacing part La of  $\text{La}_{0.67}\text{Ca}_{0.33}\text{MnO}_3$  by Bi, we observed completely different behaviors. First, the compound stays at two definitely different resistive states for the warming and cooling runs. The system stays at the high resistive state near room temperature, and switches to the low resistive state during cooling. Second, a re-entrance of the high resistivity state takes place when the sample was kept at a low temperature, showing a strong tendency to CO.

A polycrystalline sample of  $\text{La}_{0.477}\text{Bi}_{0.193}\text{Ca}_{0.33}\text{MnO}_3$  (LBCM51) was prepared by the solid-state reaction method

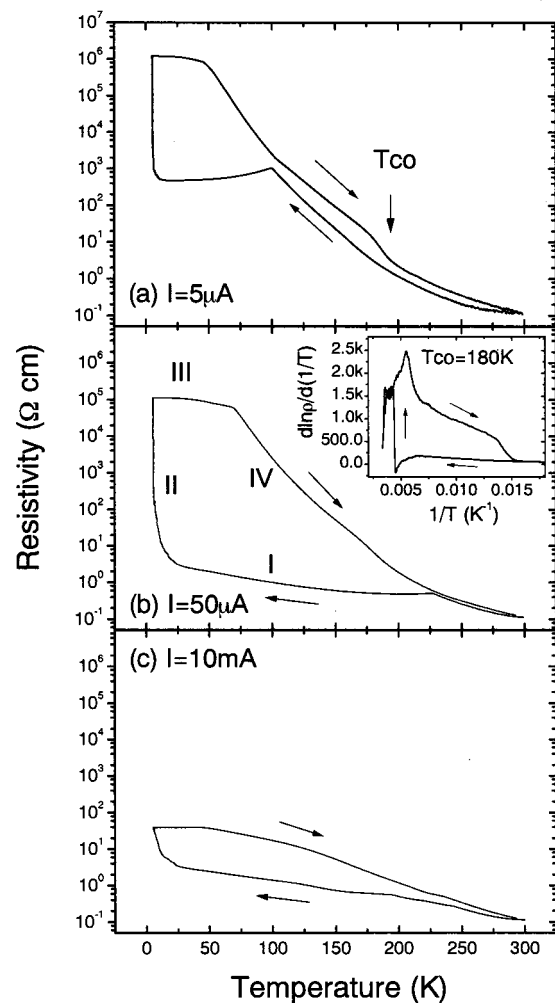


FIG. 1. Temperature-dependent resistivity measured under different applied currents. Current-dependent thermal hysteresis appears for a cooling-warming cycle. Inset of (b) shows the derivative of  $\ln \rho$  with respect to  $1/T$ .  $T_{co}$  indicates the temperature for charge ordering.

<sup>a)</sup>Author to whom correspondence should be addressed; electronic mail: jrsun@g203.iphys.ac.cn

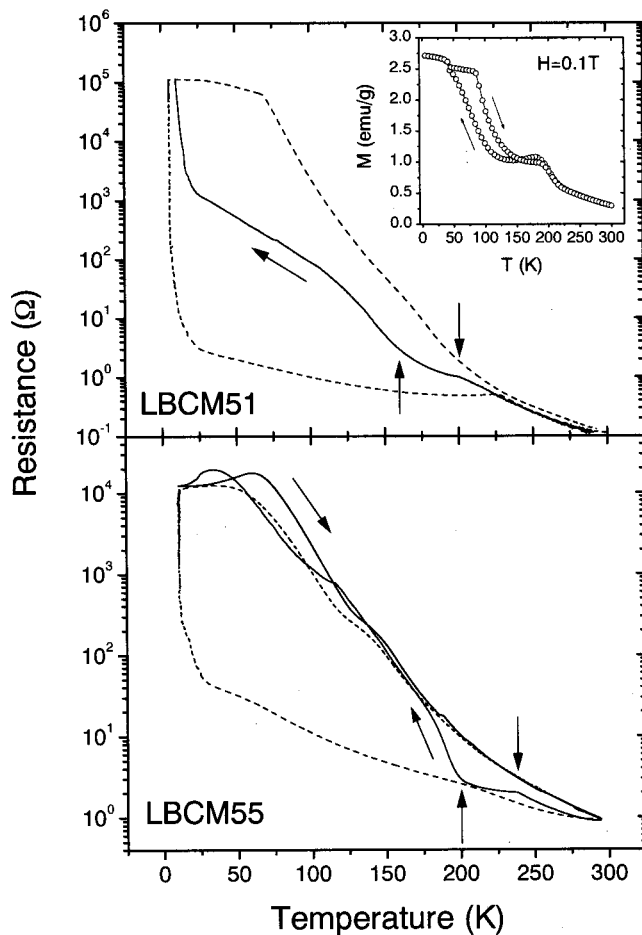


FIG. 2. Back and forth switching between different resistive states of  $\text{La}_{0.477}\text{Bi}_{0.193}\text{Ca}_{0.33}\text{MnO}_3$  (LBCM51, top panel) and  $\text{La}_{0.477}\text{Bi}_{0.193}\text{Ca}_{0.33}\text{Mn}_{0.986}\text{Cr}_{0.014}\text{O}_3$  (bottom panel). Dashed lines show the most favorable behaviors for a cooling–warming cycle. Inset displays the magnetization of LBCM51 measured under a field of 0.1 T. Arrows indicate the temperatures where the transitions occur.

following a similar procedure described elsewhere.<sup>5</sup> X-ray diffraction shows that the sample is single phase with an orthorhombically distorted perovskite structure. The lattice parameters are  $a=5.453 \text{ \AA}$ ,  $b=5.451 \text{ \AA}$ , and  $c=7.691 \text{ \AA}$ , slightly smaller than that of  $\text{La}_{0.67}\text{Ca}_{0.33}\text{MnO}_3$  (5.484, 5.471, and  $7.728 \text{ \AA}$ ).<sup>4,5</sup>

The resistance was measured by the conventional four-probe technique as a function of temperature. Indium solder was used for the connection of the lead lines to the sample. Figure 1 shows the temperature-dependent resistivity [ $\rho(T)$ ] of LBCM51. The resistivity was first measured under an applied current of  $I=5 \mu\text{A}$ . As expected, an activation-type conduction is observed when the sample was cooled below room temperature. There is a small kick in the  $\rho(T)$  curve, which is especially obvious in the warming run and is a sign of CO. All these are behaviors similar to those observed in the Pr/Nd-doped compound, and can be understood in the picture of the emergence and development of the resistive charge-ordered phase. The insulating behavior is interrupted at  $\sim 100 \text{ K}$  by an abrupt turn, and a steady resistivity decrease occurs with further cooling until  $T=7 \text{ K}$ , the lowest temperature for the present experiment. Keeping the sample at  $7 \text{ K}$ , however, a relaxation process appears, which drives

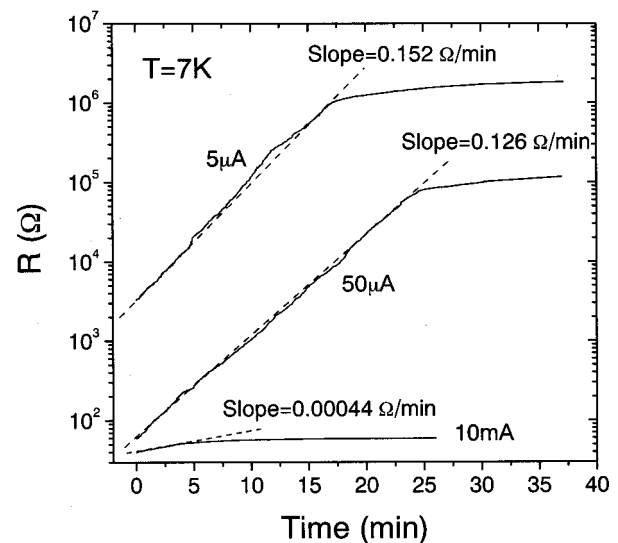


FIG. 3. Resistivity relaxation at  $T=7 \text{ K}$  under different applied currents. Resistivity increases exponentially vs time in the initial stage of the relaxation with the rate depending on the applied current.

the system to the high resistivity state again. On warming, the system first goes back to the original state, from which it deviates due to the resistive transition at  $\sim 100 \text{ K}$ , via an intermediate plateau, then runs along the  $\rho(T)$  trajectory of that state, displaying a significant thermal hysteresis.

The rigid transition at  $\sim 100 \text{ K}$  could be intrinsic for that it is repeated and a similar behavior is also observed when the applied current changes. It may not be the ordinary MI transition occurring in  $\text{La}_{1-x-y}(\text{Pr}/\text{Nd})_y\text{Ca}_x\text{MnO}_3$ . The latter is much softer and gentler. This behavior is usually expected when the system experiences a switch between two states. Subsequent experiment does suggest the presence of two resistive states. As shown in Fig. 1(b),  $\rho(T)$  goes along two definitely different routes for a cooling–warming cycle in the case  $I=50 \mu\text{A}$ . In addition to the ordinary high resistivity state observed previously (marked by IV), a state with a much smaller semiconducting slope appears below  $220 \text{ K}$  during cooling (I). The difference between these two states is also obvious from the derivative of  $\ln \rho$  with respect to  $1/T$ . A sharp maximum appears at  $\sim 180 \text{ K}$  in the warming run, indicating the enhancement of activation energy of the conduction due to the appearance of CO. This result is consistent with the neutron diffraction data that confirm the appearance of a charge-ordered antiferromagnetic structure below  $\sim 180 \text{ K}$  (not shown). In contrast, no obvious resistive anomaly is observed on cooling [inset to Fig. 1(b)]. From the above analysis, it becomes clear that the system stays at the high resistivity state initially, and transits to a low resistivity state when it is cooled.

Competition between the two states could be strong, which is apparent from the back and forth switching of the system between states. Repeating the  $\rho(T)$  measurements under an applied current of  $I=50 \mu\text{A}$ , occasionally we observed two subsequent resistive transitions during cooling, although the most frequently occurring behaviors are those presented in Fig. 1(b). As shown in the top panel of Fig. 2, the transition at  $\sim 200 \text{ K}$  shows a strong tendency of the system to the low resistivity state. However, the succeeding

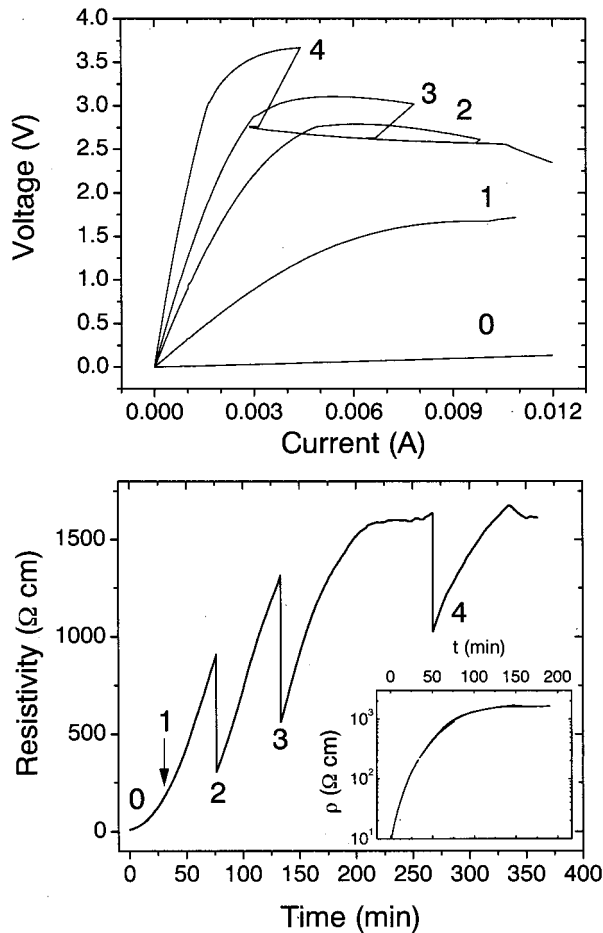


FIG. 4. Current–voltage characteristics for  $\text{La}_{0.477}\text{Bi}_{0.193}\text{Ca}_{0.33}\text{MnO}_3$  at different stages of the resistivity relaxation at 50 K (top panel) and the effects of current on resistivity (bottom panel). Inset in the bottom panel is a plot showing the universality of the relaxation behavior. Numbers in the figure indicate the times of the  $I$ – $V$  measurement.

transition at  $\sim 160$  K drives the system back to the high  $\rho(T)$  state again. This behavior is significant when minor Mn ions are replaced by Cr (bottom panel of Fig. 2). It implies that the population of the system at one state does not absolutely overwhelm that at the other.

Further studies indicate that the applied current determines whether or not the two resistive states occur. It is expected that the most favorable state will be the high  $\rho$  state in the limit without current, as occurred in the case of Pr/Nd doping, which is consistent with the experimental results in which only a weak magnetic order appears in LBCM51 for both cooling and warming runs (inset to Fig. 2). Two resistivity states appear at  $I=5\ \mu\text{A}$ , well developed for  $I=50\ \mu\text{A}$ , and are severely depressed when  $I=1\ \text{mA}$  (not shown). Only the low  $\rho$  state survives when the current exceeds 10 mA. The crucial impact of current can also be seen from the relaxation behavior of resistivity at low tempera-

ture. Though both 5 and 50  $\mu\text{A}$  are small currents, they cause different relaxation rates. The latter slows down the relaxation significantly (Fig. 3). The  $I$ – $V$  relation is a direct measure of the current effects. Figure 4 exemplifies the  $I$ – $V$  characteristics at different stages of the resistivity relaxation at 50 K. The  $I$ – $V$  dependence is linear when the resistivity is small. A nonlinear  $I$ – $V$  relation emerges when  $\rho(T)$  exceeds  $\sim 170\ \Omega\ \text{cm}$ . In this case, an irreversible resistivity change takes place. The significantly depressed resistivity does not recover after removal of the current.

As a supplement, we would like to point out that the relaxation takes place at temperatures below 60 K, and the relaxation rate depends exclusively on the initial resistivity. By applying a large current, we can depress  $\rho(T)$ , and study the relaxation starting at different initial  $\rho(T)$ . We found that all the resistivity–time relations collapse into a master curve after a proper shift of the starting time for the relaxation. This is an amazing observation considering the fact that a filament-like path is usually possible when the current pushes its way through the charge-ordered background.

In summary, the transport and magnetic properties of  $\text{La}_{0.477}\text{Bi}_{0.193}\text{Ca}_{0.33}\text{MnO}_3$  have been experimentally studied. Different resistive behaviors are observed in the cooling and warming processes. The system first stays at a high resistivity state, and switches to a state of lower resistivity when it is cooled below a critical temperature. However, keeping the sample at a temperature below  $\sim 60$  K, relaxation to the high resistive state takes place. This process is current dependent, and the application of a large current slows down the relaxation greatly. The system shows a tendency to switch between different states, which implies strong competition between the two resistive states.

This work was supported by the State Key Project for Elementary Research of China and the National Science Foundation of China.

- <sup>1</sup>S. Jin, T. H. Tiefel, M. McCormack, R. A. Fastracht, R. Ramesh, and L. H. Chen, *Science* **264**, 413 (1994).
- <sup>2</sup>P. Shiffer, A. P. Ramirez, W. Bao, and S.-W. Cheong, *Phys. Rev. Lett.* **75**, 3336 (1995).
- <sup>3</sup>J. M. De Teresa, M. R. Ibarra, I. Bosco, J. Garía, C. Marquina, P. A. Algarabel, Z. Arnold, K. Kamenev, C. Ritter, and R. von Helmolt, *Phys. Rev. B* **54**, 1187 (1996).
- <sup>4</sup>J. Bosco, J. Garcia, J. M. De Teresa, M. R. Ibarra, P. A. Algarabel, and C. Marquina, *J. Phys.: Condens. Matter* **8**, 7427 (1996).
- <sup>5</sup>G. H. Rao, J. R. Sun, J. K. Liang, and W. Y. Zhou, *Phys. Rev. B* **55**, 3742 (1997).
- <sup>6</sup>M. Uehara, S. Mori, C. H. Chen, and S.-W. Cheong, *Nature (London)* **399**, 560 (1999); K. H. Kim, M. Uehara, C. Hess, P. A. Sharma, and S.-W. Cheong, *Phys. Rev. Lett.* **84**, 2961 (2000); V. Podzorov, M. E. Gershenson, M. Uehara, and S.-W. Cheong, *Phys. Rev. B* **64**, 115113 (2001).
- <sup>7</sup>T. Kimura, Y. Tomioka, R. Kumai, Y. Okimoto, and Y. Tokura, *Phys. Rev. Lett.* **83**, 3940 (1999); Y. Tomioka, A. Asamitsu, H. Kuwahara, and Y. Tokura, *Phys. Rev. B* **53**, R1689 (1996).
- <sup>8</sup>H. Woo, T. A. Tyson, M. Croft, S.-W. Cheong, and J. C. Woicik, *Phys. Rev. B* **63**, 134412 (2001).

Applied Physics Letters is copyrighted by the American Institute of Physics (AIP). Redistribution of journal material is subject to the AIP online journal license and/or AIP copyright. For more information, see <http://ojps.aip.org/aplo/aplcr.jsp>  
Copyright of Applied Physics Letters is the property of American Institute of Physics and its content may not be copied or emailed to multiple sites or posted to a listserv without the copyright holder's express written permission. However, users may print, download, or email articles for individual use.